

DMD/2016/071639

**The Use of *In vitro* Data and Physiologically-Based Pharmacokinetic Modeling to
Predict Drug Metabolite Exposure: Desipramine Exposure in Cytochrome P4502D6
Extensive and Poor Metabolizers Following Administration of Imipramine**

Hoa Q. Nguyen, Ernesto Callegari, and R. Scott Obach

Department of Pharmacokinetics, Dynamics, and Metabolism, Pfizer Global Research and Development,
Groton, Connecticut, USA

DMD/2016/071639

Running Title: Prediction of Drug Metabolite Exposure

Corresponding Author:

Hoa Q. Nguyen. Mailing Address: Department of Drug Metabolism and Pharmacokinetics. R&D 1521.

Boehringer Ingelheim, 900 Ridgebury Road, Ridgefield, Connecticut, 06877. Office telephone: 203-791-

6098. Email: hoa_2.nguyen@boehringer-ingelheim.com

Number of text pages: 30

Number of tables: 6

Number of figures: 9

Number of references: 64

Number of words in the Abstract: 248

Number of words in the Introduction: 750

Number of words in the Discussion: 1594

Abbreviations

AUC, area under the concentration-time curve; C_{max} , maximum plasma concentration; CYP, cytochrome P450 enzyme; UGT, UDP-glucuronosyltransferase; CL, clearance; $CL_{int, u, met}$, unbound metabolic intrinsic clearance; $CL_{int, pass}$, unbound passive diffusion intrinsic clearance; fu_{cell} , fraction unbound in hepatocytes; fu_p , fraction unbound in plasma; fu_{inc} , fraction unbound in incubation mixture; IS, internal standard; HLM, human liver microsomes; LC-MS/MS, liquid chromatography/tandem mass spectrometry; PBPK: physiologically-based pharmacokinetic modeling.

DMD/2016/071639

Abstract

Major circulating drug metabolites can be as important as the drugs themselves in efficacy and safety, so establishing methods whereby exposure to major metabolites following administration of parent drug can be predicted is important. In this study, imipramine, a tricyclic antidepressant, and its major metabolite desipramine were selected as a model system to develop metabolite prediction methods. Imipramine undergoes N-demethylation to form the active metabolite desipramine, and both imipramine and desipramine are converted to hydroxylated metabolites by the polymorphic enzyme CYP2D6. The objective of the present study is to determine if the human pharmacokinetics of desipramine following dosing of imipramine can be predicted using static and dynamic PBPK models from *in vitro* input data for CYP2D6 EM and PM populations. The intrinsic metabolic clearances of parent drug and metabolite were estimated using human liver microsomes (CYP2D6 PM and EM) and hepatocytes. Passive diffusion clearance of desipramine, used in the estimation of availability of the metabolite, was predicted from passive permeability and hepatocyte surface area. The predicted AUC_m/AUC_p of desipramine/imipramine was **12 to 20 fold** higher in PM compared to EM subjects following i.v. or oral doses of imipramine using the static model. Moreover, the PBPK model was able to recover simultaneously plasma profiles of imipramine and desipramine in populations with different phenotypes of CYP2D6. This example suggested that mechanistic PBPK modeling combined with information obtained from *in vitro* studies can provide quantitative solutions to predict *in vivo* pharmacokinetics of drugs and major metabolites in a target human population.

DMD/2016/071639

Introduction

Recent regulatory guidance from FDA and ICH (FDA, 2008; Guideline, 2009) propose that any drug metabolite with exposure > 10% of the parent or of the total drug-related material exposure at steady-state in humans warrants further consideration with regard to safety. These guidelines recommend identifying the metabolic profile of the drug in humans, and determining systemic exposure of relevant metabolites (AUC_m) relative to parent (AUC_p) in clinical and non-clinical studies. The metabolite/parent area under the plasma concentration versus time curve ratio (AUC_m/AUC_p) is also a commonly used metric in drug interaction studies involving metabolites (Callegari et al., 2013; FADA, 2012; Guideline, 2012; Yeung et al., 2011; Yu and Tweedie, 2013).

The establishment of drug metabolite kinetic principles dates back to the 1980s (Houston and Taylor, 1984; Houston, 1981; Pang, 1985; St-Pierre et al., 1988). However, while the use of *in vitro* studies to predict *in vivo* pharmacokinetics of drugs is commonplace, the use of these approaches to predict pharmacokinetics of metabolites has not been thoroughly established due to the number of contributing variables on metabolite exposure. The equations developed by Houston (Houston, 1981) for the metabolite/parent ratio (AUC_m/AUC_p) represent “static” models, which provides conceptual insight as to the determinants of metabolite exposure including the clearance rate of the parent drug, the fraction of the dose of the parent drug that is converted to the metabolite, and the subsequent clearance of the metabolite. Another factor can also impact metabolite disposition is its systemic availability following formation from parent drug, which depends upon sequential elimination, permeability, and transport properties of the metabolite.

A different approach to the understanding of circulating metabolite *in vivo* PK behavior is utilizing *in vitro* data of parent drug and metabolites in integrated dynamic PBPK models. PBPK is also

DMD/2016/071639

potentially of value as a tool to evaluate the effect of various population factors on pharmacokinetic outcomes including genetic polymorphism (Jamei et al., 2009; Rowland et al., 2011; Vieira et al., 2014).

In the present study, desipramine, an active metabolite of the tricyclic antidepressant imipramine, was selected as a test case to apply the approach of integrating *in vitro* data into static and dynamic PBPK models for metabolite exposure prediction following administration of parent drug, which was proposed in the previous study (Nguyen et al., 2016). Both imipramine and desipramine were demonstrated to undergo hydroxylation catalyzed by CYP2D6 (Brøsen and Gram, 1988; Sallee and Pollock, 1990). The pharmacokinetic implications resulting from genetically determined variability in the expression of CYP2D6 may cause clinical significance in depression treatment with desipramine and imipramine (Dahl et al., 1992; Furman et al., 2004; Schenk et al., 2008). In this study, the impact of CYP2D6 polymorphism on metabolism and disposition of both parent drug and metabolite was investigated by simulating time-course profiles in populations of CYP2D6 extensive metabolizer (EM) and poor metabolizer (PM) genotypes. *In vitro* data were generated for imipramine and desipramine including metabolic intrinsic clearance, protein binding, and membrane permeability. These data were used as input values for static and PBPK models in CYP2D6 EM and PM subjects, and compared to the PK parameters reported in the literature.

DMD/2016/071639

Materials and Methods

Materials

Imipramine, desipramine, and amitriptyline hydrochloride were purchased from Sigma Chemical Co. Pooled human liver microsomes (lot number HLM102, a mixture of both genders, CYP2D6 extensive metabolizer phenotype) were prepared under contract from BD Biosciences, Woburn, MA. **CYP2D6 poor metabolizer HLMs (lot HH35, HH79, 413, 499, and 486) were purchased from BD Gentest™ (New Jersey, NJ) and Xenotech (Kansas, KS) and pooled.** Cryopreserved human hepatocytes (N=10 donors, mixed gender) were purchased from *In vitro* ADMET Laboratories (Columbia, MD). Other reagents and solvents used were from standard suppliers and were of reagent or HPLC grade.

Metabolite Profile of Imipramine in Hepatocytes

In vitro incubation: Human hepatocyte ($\sim 0.75 \times 10^6$ cells/mL) incubations were performed in Williams E medium in a total volume of 1 mL using 10 μ M of imipramine concentration. Incubations were conducted at 37 °C under a gas mixture of 5% CO₂ /95% O₂. At time zero, 500 μ L of sample was quenched with 2.5 mL of CH₃CN. At time 30 and 60 min, 250 μ L of sample at each time was added to the same volume of 2.5 mL CH₃CN. The precipitate was removed by centrifugation (1700g) for 5 min, the supernatant was decanted into a 15 mL conical glass tube, and the liquid was evaporated under a stream of nitrogen at 35 °C using Genevac evaporator. The resulting residue was reconstituted in 0.1 mL of water containing 1% HCOOH for HPLC-UV-MS/MS analysis.

Metabolite Identification: The imipramine human hepatocyte extracts were analyzed by UHPLC-UV-MS on a Thermo Orbitrap Elite coupled with Accela HPLC pump, photodiode array detector, and CTC Leap autoinjector (Thermo Fisher Scientific, Waltham, MA). Separation was effected on an Acquity BEH C18 column (2.1x100mm; 1.7 μ m particle size) using a mobile phase consisting of 0.1% HCOOH in water (A) and CH₃CN (B) at a flow rate of 0.4 mL/min. The mobile phase composition began at 5%B, held for

DMD/2016/071639

0.5 min, increased linearly to 40% B at 6 min, increased linearly to 80% B at 8 min, followed by a 1 min wash at 95%B and 1.5 min re-equilibration to initial conditions. The effluent passed through the PDA detector scanning from 200-400 nm and then into the source of the mass spectrometer operated in the positive ion mode. The source temperature was set at 400°C and other settings and potentials were adjusted to maximize the signal for the protonated molecular ion of imipramine. The injection volume was 10 μ L.

Metabolites formed in the hepatocyte incubation of imipramine were identified using UV and total ion chromatograms. The UV chromatograms were reconstructed using the wavelength maxima of the parent compound. These were then compared to UV chromatograms of the corresponding control incubation without parent drug. The UV peaks that were only present in the chromatograms of the incubation mixture but absent in the controls were identified as potential metabolites of imipramine. These were integrated and the f_m for desipramine formation from imipramine was estimated as the desipramine peak area divided by the sum of peak areas for all observed imipramine metabolites.

Enzyme Kinetic Study of Imipramine Metabolism in Hepatocytes

A preliminary experiment was conducted to determine linearity with respect to incubation time and hepatocyte concentration, wherein product formation was measured following substrate incubation at several different time points (2 – 45 min) and at several different hepatocyte concentrations (0.25 – 1×10^6 cells/mL). For incubation, 30 μ L of cell suspensions was added to a 96-well polystyrene plate with lid and incubated under a gas mixture of 5% CO₂ /95% O₂ for 30 minutes. After preincubation, the reaction was commenced by adding 15 μ L of imipramine stock solutions prepared in Williams E medium and maintained at 37°C in incubator for 10 min. The final hepatocyte concentration was 0.25×10^6 cells/mL and the final substrate concentration ranged from 0.5 to 400 μ M. All hepatocyte incubations were quenched by the addition of 135 μ L of acetonitrile containing internal standard (amitriptyline 0.05

DMD/2016/071639

μM), and centrifuged at 3000 rpm for 10 min. Supernatant was transferred to a clean 96-well plate for LC-MS/MS analysis. The experiments were performed in triplicate.

The *in vitro* data were initially transformed for Eadie-Hofstee plot to assess linearity and diagnose appropriate enzyme kinetic models for the data. Kinetic parameters, V_{max} and K_m , were estimated by fitting the selected model to the *in vitro* data using nonlinear regression in GraphPad Prism (version 6.03).

CL_{int} Determination of Desipramine in CYP2D6 EM and PM Microsomes

The intrinsic clearance (CL_{int}) of desipramine was determined in triplicate using human liver microsomes (EM HLM). Microsomes (0.5 mg/ml) were preincubated for 5 min at 37°C in 100 mM KH₂PO₄, pH 7.4, containing 3.3 mM MgCl₂, and 1.3 mM NADPH. The reactions were initiated by adding pre-warmed test compound (1 μM final concentration of desipramine). After zero, 5, 10, 20, 30, 45 and 60 min post-commencement of the incubation, the reactions were stopped by adding a 4-fold volume of acetonitrile containing 0.05 μM of amitriptyline (internal standard). The samples were centrifuged at 3000g for 10 min. The supernatants were analyzed with LC/MS/MS for the amount of parent compound remaining.

Intrinsic clearance of desipramine in CYP2D6 poor metabolizer HLMs **using a pool of five CYP2D6 PM donors** was determined in similar experimental procedure, except that the incubation mixture included 1 mg/mL of pooled PM HLMs.

Calculation of apparent intrinsic clearance was done using the following equation:

$$CL_{int} = \frac{0.693}{t_{1/2} \times C_{protein}} \times \frac{45 \text{ mg microsomal protein}}{\text{g of liver weight}} \times \frac{20 \text{ g of liver}}{\text{kg body weight}} \quad (\text{Eq. 1})$$

where $C_{protein}$ is the microsomal protein concentration in incubation mixture, the *in vitro* elimination half-life $t_{1/2}$ was determined from the slope (-k) of the linear regression from log percentage remaining versus incubation time relationships ($t_{1/2} = -0.693/k$).

DMD/2016/071639

CL_{int} determination of Imipramine in Hepatocytes

CL_{int} of imipramine determinations in hepatocytes were performed in triplicate, in William E medium, pH 7.4, with final 0.5×10^6 hepatocytes/ml and 1 μ M imipramine. The incubations were carried out in a 37°C 5% CO₂/95% O₂ incubator. The reactions were stopped at 0, 5, 15, 30, 60, 120 and 240 minutes with the addition of 3-fold volume of acetonitrile containing 0.05 μ M amitriptyline. The values of 0.5×10^6 hepatocytes/ml and 120×10^6 hepatocytes/g liver for humans (Naritomi et al., 2003) were used in the imipramine CL_{int} calculation (Eq. 1).

Protein Binding ($f_{u,inc}$, $f_{u,p}$, $f_{u,cell}$)

Microsomes (0.5 mg/mL) were mixed with 1 μ M of test compound in 100 mM KH₂PO₄, pH 7.4 and MgCl₂ (3.3 mM). The mixtures (150 μ L) were loaded into the donor compartment of the equilibrium dialysis device. Aliquots of corresponding blank buffer mix (150 μ L) were placed into the receiver compartments. Dialysis experiments were performed in quadruplicate. After 4 hours of incubation in an incubator (5% CO₂, 75% relative humidity) on a shaker, the microsomes and buffer samples were removed. Microsomal samples (15 μ L) were mixed with control buffer (45 μ L), and buffer samples (45 μ L) were mixed with control microsomes (15 μ L) to yield an identical matrix before samples were precipitated by 180 μ L cold acetonitrile containing 0.05 μ M amitriptyline (IS). After centrifugation, supernatant was withdrawn for HPLC-MS analysis. Drug recovery and stability through the dialysis procedure was also determined by analyzing samples of the mixtures that were not subjected to dialysis. The free fraction in microsomal incubations ($f_{u,inc}$) was calculated from the concentrations of test compound in donor and receiver compartments.

The plasma protein fraction unbound ($f_{u,p}$) was determined using a similar procedure, except that plasma was thawed and adjusted to pH 7.4 **with 1N HCl** before the addition of test compounds.

The fraction unbound in hepatocytes ($f_{u,cell}$) was calculated using equation 2 reported by Jones et al (Jones et al., 2012), assuming that the concentration of macromolecules (e.g. albumin, globulins

DMD/2016/071639

and lipoproteins) in liver relative to that in plasma ($C_{m_{tissue}}/C_{m_{plasma}}$) is equal to 0.5 (Poulin and Theil, 2000).

$$f_{u_{cell}} = \frac{1}{1 + \left(\frac{1 - f_{u_p}}{f_{u_p}}\right) \times \frac{C_{m_{tissue}}}{C_{m_{plasma}}}}$$

Prediction of Passive Diffusion Clearance

The rate of total mass transport across a cellular membrane (dM_{pass}/dt) by passive transport can be described by equation below (Sugano et al., 2010):

$$\frac{dM_{pass}}{dt} = A \times P_{pass} \times C \quad (\text{Eq. 3})$$

Where A is the surface area of a membrane (length^2); P is the permeability ($\text{length}/\text{time}$); C is the concentration of a permeant ($\text{amount}/\text{length}^3$).

Hence, the hepatic passive transport clearance (product of $A \times P_{pass}$) can be predicted from passive permeability and hepatocyte surface area, as follows:

$$CL_{int,pass} = \text{Passive permeability} \times \text{Hepatocyte Cell Surface Area} \times N \text{ cells} \quad (\text{Eq. 4})$$

where passive permeability of desipramine is experimentally measured PAMPA permeability from Fujikawa et al (Fujikawa et al., 2007) ($P_{PAMPA} = 17.0 \times 10^{-6} \text{ cm/s}$). Human hepatocyte cell surface area is $1.6 \times 10^{-5} \text{ cm}^2$ (Chen et al., 2005). Number of cells is product of 120×10^6 cells /gram liver (Naritomi et al., 2003) and 20 g liver/kg body weight.

Prediction of metabolite systemic availability

Following its formation from imipramine in liver, the systemic availability (F_m) of desipramine was estimated based on the well-stirred model (Houston, 1981) which was modified to incorporate the interplay between passive diffusion ($CL_{int,pass}$), hepatic blood flow (Q_h), and metabolic intrinsic clearance of desipramine ($CL_{int,u,met}$), assuming no or negligible involvement of hepatic transporters:

DMD/2016/071639

$$F_m = \frac{\frac{Q_h \times CL_{int,pass}}{Q_h + CL_{int,pass}}}{\frac{Q_h \times CL_{int,pass}}{Q_h + CL_{int,pass}} + fu_B \times CL_{int,u,met}} \quad (\text{Eq. 5})$$

Where hepatic blood flow (Q_h) is ~ 21 mL/min/kg. The free fraction in blood (fu_B) is the free fraction in plasma (fu_p) corrected by the blood-to-plasma ratios, which are 1.02 and 1.16 for imipramine and desipramine, correspondingly obtained as the mean values from resources including Simcyp library and literature (Ciraulo et al., 1988; Fišar et al., 1996; Obach, 1997; 1999). $CL_{int,pass}$ and $CL_{int,u,met}$ are intrinsic passive diffusion and metabolic clearances, respectively.

Static Model of AUC_m/AUC_p

The *in vivo* ratios of area under the plasma concentration-time curve of metabolite versus parent drug after intravenous and oral administration of parent can be described by the following equations (Houston, 1981):

After an i.v. dose of parent drug:

$$\frac{AUC_m}{AUC_p} = \frac{F_m \times f_{CL,m} \times CL_p}{CL_m} \quad (\text{Eq. 6})$$

After an oral dose of parent drug:

$$\frac{AUC_m}{AUC_p} = \frac{F_m \times f_{CL,m} \times CL_p}{F_h \times CL_m} \quad (\text{Eq. 7})$$

in which, $f_{CL,m}$ is the fraction of the clearance of the parent drug that yields the metabolite. F_m , the metabolite systemic availability, is the portion of the total metabolite generated within an organ that is released into the systemic circulation before it is either further metabolized or secreted into bile. CL_p is the total clearance of the parent drug, and CL_m is the total clearance of the metabolite. In equation 7, the fraction of imipramine that escapes first-pass elimination in the liver was estimated from *in vitro* total clearance of parent:

DMD/2016/071639

$$(F_h = 1 - \frac{CL_p}{Q_h}) \quad (\text{Eq. 8})$$

In the static model for CYP2D6 EMs, the fraction of imipramine converted to desipramine, $f_{CL,m}$, was estimated based on imipramine metabolic profile determined from EM hepatocyte *in vitro* system. For PMs, desipramine $f_{CL,m}$ of 0.8 was obtained from clinical data of Brosen and Gram (Brøsen and Gram, 1988).

The total body clearance values of parent and metabolite were predicted from *in vitro* intrinsic metabolic clearances (EM and PM HLM) using the well-stirred model as follows:

$$CL_p = \frac{Q_h \times fu_{B,parent} \times CL_{int,u,parent}}{Q_h + fu_{B,parent} \times CL_{int,u,parent}} \quad (\text{Eq. 9})$$

$$CL_m = \frac{Q_h \times fu_{B,metab} \times CL_{int,u,metab}}{Q_h + fu_{B,metab} \times CL_{int,u,metab}} \quad (\text{Eq. 10})$$

PBPK Modeling and Simulations

Modeling and simulations of imipramine and its metabolite desipramine were performed using the population-based ADME simulator Simcyp (version 14; Simcyp Ltd., Sheffield, United Kingdom). Simulations were performed for two virtual populations of 500 (10 trials x 50 subjects each) healthy volunteers aged between 20 and 50 with a Male/Female ratio of 50/50, in fasted conditions, representing PM- and EM- CYP2D6 individuals receiving a normalized dose of 1 mg imipramine intravenously or orally. The PM population was generated by setting the frequency of PM CYP2D6 phenotype as 1, and other phenotypes (IM, UM and EM) as 0 in demographic of trial design. Meanwhile, CYP2D6 phenotype PM, IM, UM frequencies were set to 0 for EM population.

For imipramine, a minimal PBPK model was developed assuming perfusion-limited distribution and using the physicochemical (pKa, logP), biochemical properties (human plasma f_u , blood-to-plasma ratio) and *in vitro* metabolic intrinsic clearance values (Table 1). The PBPK model for desipramine was similar to its parent drug, using desipramine physicochemical and intrinsic clearance parameters (Table

DMD/2016/071639

1). The volumes of distribution at steady-state (V_{ss}) were 11 and 6.5 L/kg, for imipramine and desipramine, respectively. These values were predicted using the model proposed by Rodgers and Rowland (Rodgers and Rowland, 2006). For imipramine metabolism, enzyme kinetic information using *in vitro* human hepatocytes data was used. The unit of $\mu\text{L}/\text{min}/10^6$ cells was converted to $\mu\text{L}/\text{min}/\text{mg}$ protein using conversion factors of 120×10^6 cells/g liver and 45 mg microsomal protein/g liver (Zhang and Kaminsky, 2007). CL_{int} value of 9.12 $\mu\text{L}/\text{min}/\text{mg}$ protein for N-demethylation pathway was used after taking the sum of two enzyme kinetic parameters (V_{max}/K_m and CL_{int2}). The value of 8 $\mu\text{L}/\text{min}/10^6$ cells was assigned for additional clearance to account for other pathways by subtracting N-demethylation CL_{int} from total intrinsic clearance of imipramine. For desipramine metabolism, CL_{int} of 22.0 $\mu\text{L}/\text{min}/\text{mg}$ protein was assigned to account for hydroxylation pathway by CYP2D6.

HPLC-UV-MS/MS Method for Quantitation of Imipramine and Desipramine

Analyses of substrate and metabolites were performed using high-performance liquid chromatography (Agilent model 1290 binary pump) followed by tandem mass spectrometry (Triple Quad 5500; Applied Biosystems/Sciex, Thornhill, Ontario, Canada). The chromatographic separation was carried out on a Phenomenex Kinetex C18 100Å 30x2.1 mm column. Mobile phases consisted of 0.1% formic acid in water (mobile phase A) and 0.1% formic acid in acetonitrile (mobile phase B), and was delivered at 0.5 mL/min. The initial composition of solvent B was maintained at 10% for 0.8 min, then increased to 90% after 1.2 min, and returned to 10% after 1.7 min, and held (2.0 min total). The injection volume was 10 μL . The TurbolonSpray interface was operated in the positive ion mode at 5500 V and 500°C. Quadrupoles Q1 and Q3 were set on unit resolution. Multiple-reaction-monitoring mode using specific precursor/product ion transitions was used for quantification. Detection of the ions was performed by monitoring the transitions of mass/charge ratio (m/z) with collision energy of 30 eV as follows: imipramine (281.2 \rightarrow 86); desipramine (267 \rightarrow 208); and amitriptyline (internal standard, IS) (278.4 \rightarrow 91).

DMD/2016/071639

Stock solutions of imipramine, desipramine and internal standard (amitriptyline) were prepared in methanol. Desipramine was quantitated from standard curve ranging from 0.5 – 1000 nM. Data processing was performed using Analyst™ software (version 1.6.2, Sierra Analytics LLC).

DMD/2016/071639

Results

Metabolite Profile of Imipramine in Human Hepatocytes to Estimate f_m Values

The metabolism of imipramine was assessed in human hepatocyte incubations. Chromatograms (UV traces) are shown in Figure 1 and corresponding fractional conversion from parent drug f_m are listed on Table 2 and Figure 2. A total of four major metabolites were observed in this *in vitro* incubation. Primary metabolic pathways of imipramine produced desipramine (m/z 267), hydroxy imipramine (m/z 297) and imipramine N-glucuronide (m/z 457). Hydroxy desipramine may be formed from sequential metabolism of desipramine or demethylation of hydroxy imipramine. Due to this, the fractional conversion from imipramine via N-demethylation pathway ($f_{cl,m}$) was estimated as a range from 0.44 to 0.62. The fraction of imipramine that undergoes hydroxylation is in the range of 0.20 – 0.38. These ranges reflect extreme cases, i.e that hydroxy desipramine arose 100% via desipramine or 100% via hydroxy imipramine. Glucuronidation is responsible for 0.18 fraction of imipramine metabolism.

Enzyme Kinetic Parameters of Desipramine Formation

The enzyme kinetics of metabolism of imipramine to desipramine was studied in human hepatocytes. The velocity of N-demethylation was investigated using imipramine at final concentrations from 0.5 to 400 μ M. The kinetic data are shown in Figure 3 and indicate that at least two distinct enzymes are responsible for demethylation pathway. The Eadie-Hofstee plot (Figure 3) showed that demethylation exhibited biphasic kinetics. Therefore, the total velocity for desipramine formation was described by two-enzyme model as follows:

$$v = \frac{V_{max} \times C}{K_m + C} + CL_{int2} \times C \quad (\text{Eq. 11})$$

where V_{max} and K_m are the apparent maximal velocity and the apparent Michaelis constant, respectively, of low K_m enzyme, and CL_{int2} is the intrinsic clearance representing the high K_m site. The best fit values of V_{max} , K_m and CL_{int2} were shown in Figure 3.

DMD/2016/071639

***In vitro* CL_{int} of Imipramine in Hepatocytes and Desipramine in Liver Microsomes**

The apparent intrinsic clearance values of imipramine and its active metabolite, desipramine were calculated from the degradation rate constants in their corresponding depletion curves (Figure 4 and 5). For desipramine, human liver microsomes were used since the metabolic clearance of desipramine is mediated mainly by cytochrome P450, while for imipramine this measurement was made in human hepatocytes since glucuronidation is also a component of clearance (Nakajima et al., 2002; Zhou et al., 2010). These apparent values were corrected for nonspecific binding of test compounds within microsomal (desipramine $f_{u_{mic}} = 0.39$) and hepatocyte (imipramine $f_{u_{cell}} = 0.42$) incubations. Apparent intrinsic clearances and protein binding of imipramine and desipramine are displayed in Figure 4 and 5, respectively. Intrinsic clearance of $2.5 \pm 0.9 \mu\text{L}/\text{min}/\text{mg}$ protein of desipramine obtained in CYP2D6 poor metabolizer HLMs was also determined, which is **about 9-fold lower** than the value obtained from EM HLM incubations ($22 \pm 1.4 \mu\text{L}/\text{min}/\text{mg}$ protein). **However this estimate possesses uncertainty since the depletion of desipramine in PM liver microsomes is low.**

CL, CL_{int,pass} and F_m Predictions

Table 3 shows the predicted total clearance of parent drug (CL_p) and desipramine (CL_m), F_h of parent drug, as well as intrinsic passive diffusion (CL_{int,pass}) and systemic availability (F_m) of desipramine. The predicted total clearance of imipramine is 9.4 mL/min/kg and clearance values of desipramine are 6.4 and **1.0** mL/min/kg for EMs and PMs, respectively. About 55% of imipramine presented in the liver was predicted to escape the first-pass metabolism after an oral dose. Following its formation from imipramine, 60% of desipramine was estimated to leave the liver and reach the systemic circulation in EM populations. Due to its decreased activity of CYP2D6 isozyme in PMs, desipramine elimination rate is decreased, leading to increased systemic availability of this metabolite in circulation (**93%**) (Table 3).

DMD/2016/071639

AUC_m/AUC_p

The predicted total clearance (CL_p and CL_m), fractional conversion from parent drug (f_m), F_h and F_m were used as input parameters to predict the relative exposure of desipramine compared to parent drug after i.v and oral administration of imipramine to extensive and poor metabolizer CYP2D6 healthy populations, using equations 6 and 7. For EM populations, the predicted AUC_m/AUC_p ratios are consistent with clinical data shown in Table 4. The data highlighted the clinical relevance of the CYP2D6 oxidation polymorphism in the pharmacokinetics of imipramine and desipramine. In the CYP2D6 poor metabolizers, increased desipramine plasma levels were predicted when comparing to those in extensive metabolizers. **Due to this, the estimated AUC ratio of desipramine versus imipramine was ~ 12 - 20-fold higher in PM than in EM populations, following i.v or oral dosing of parent drug in the static and PBPK models whereas, the observed AUC ratio was 6 to 14 fold higher in PM than in EM volunteers.** From PBPK simulations, the predicted mean ratios range from 0.19 to 0.28 and from 0.32 to 0.54 after i.v and oral dose of imipramine, correspondingly. In PM populations, PBPK model predicted the range of mean ratios from 3.7 to 5.0 and from 6.5 to 9.1 after i.v and oral dose of imipramine, respectively.

Concentration-time profiles of imipramine and metabolite desipramine

The predicted means for 10 trials and observed plasma concentration-time profiles of imipramine and its active metabolite desipramine after i.v infusion and oral administration of imipramine **normalized dose to 1 mg** are shown in Figure 6 – 9. Predicted PK parameters for imipramine and active metabolite desipramine are listed in Table 5 and 6. After an oral dose of 1 mg imipramine in EM, mean predicted AUC(0,∞) value of imipramine across the whole population was 13 ng/mL.hr, whereas the mean value of individual trial ranged from 12 to 15 ng/mL.hr. Mean predicted AUC(0,∞) value of desipramine was 5.8 ng/mL.hr (mean of trials ranged from 4.3 to 6.9 ng/mL.h). In CYP2D6 PMs,

DMD/2016/071639

predicted AUC(0,∞) value of desipramine for the whole population was 104 ng/mL.hr (range from 86 to 116 ng/mL.h).

DMD/2016/071639

Discussion

Understanding the potential for contribution of a metabolite(s) to drug clinical efficacy, toxicity, or DDIs can be challenging and require a thorough knowledge of drug and metabolite disposition. Development of methods to accomplish this requires testing examples of drugs and metabolites that have human pharmacokinetic data and well-understood overall disposition. The example of desipramine as a metabolite to which humans are exposed following administration of imipramine was selected for this study since human pharmacokinetics and metabolism are well known. Furthermore, since desipramine is cleared by CYP2D6, this example offers the opportunity to predict desipramine exposure after imipramine administration to two different population groups, i.e. CYP2D6 extensive and poor metabolizers.

CYP2D6 genes are highly polymorphic, which leads to wide inter-individual variation in drug clearance, induction of adverse effects and increased potential for drug–drug interactions (Bernard et al., 2006). Since desipramine is mainly metabolized by a single enzyme, CYP2D6, it been used widely as a probe drug for CYP2D6 activity (Ball et al., 1997; Kurtz et al., 1997; Madani et al., 2002; Spigset et al., 1997; Spina et al., 1997). High ratios of desipramine metabolite to parent drug due to impaired metabolism caused by the CYP2D6 PM phenotype have been related to increased frequency of adverse drug reactions, and even death, upon chronic administration of therapeutic doses (Leucht et al., 2000; Swanson et al., 1997).

In the overall metabolic profile of imipramine (Figure 2), N-demethylation is the major pathway with the highest fraction of total clearance of the parent drug ($f_{cl,m} = 0.44 - 0.62$). Potter et al. (Potter et al., 1982) demonstrated a similar finding that desipramine was the major circulating metabolite quantified in patient plasma (accounted for 67% total concentration of metabolites). By measuring the AUCs of desipramine in the PK studies whether desipramine was given as parent compound or formed

DMD/2016/071639

from imipramine, Broesen et al calculated the demethylation fraction of imipramine after the i.v. dose at 0.34 in CYP2D6 EMs and 0.67 in PMs. Likewise, this fraction slightly increased after an oral dose of imipramine: 0.53 in EMs and 0.8 in PM populations (Brøsen and Gram, 1988; Brøsen et al., 1986). In CYP2D6 PMs, the decreased activity of CYP2D6 reduces the extent of formation of hydroxyimipramine from imipramine thereby directing more of the imipramine dose to desipramine, increasing the demethylation fraction of imipramine compared with EM population. **By using the LC/UV to determine the fraction of metabolic clearance of parent that forms a specific metabolite, it is acknowledged that in the absence of a standard for the relevant metabolite, assumption of equivalent UV absorptivity needs to be made, even though modifications of the chemical structure can lead to changes in the UV absorbance relative to the parent drug.**

In order to use *in vitro* data in a bottom-up approach to predict the exposure of a drug metabolite relative to the parent drug exposure, the following parameters must be predicted: total clearance of parent drug (CL_p), total clearance of the metabolite (CL_m), the fraction of the dose of the parent drug that is converted to the metabolite (f_m), and the fraction of the metabolite that once formed can enter the systemic circulation before being cleared within its organ of generation (F_m). The use of *in vitro* metabolism in scaling to predict human clearance has been a routine practice within pharmaceutical research and development organizations (Obach, 2011). In this study, the predicted CL_p of imipramine of 9.4 mL/min/kg from *in vitro* CL_{int} was consistent with clinical values ranging from 8 to 15 mL/min/kg (Abernethy et al., 1984; Ciraulo et al., 1988; Sallee and Pollock, 1990; Sutfin et al., 1984). The observed CL_m of desipramine were 2 - 3 and 12 mL/min/kg in PM and EM populations, respectively (Brøsen and Gram, 1988; Ciraulo et al., 1988) and in the present study, CL_m of desipramine was reasonably predicted as 1.0 mL/min/kg from *in vitro* CL_{int} using HLM of PM donors and 6.4 mL/min/kg using EM HLMs. The f_m value was estimated from metabolite profiling experiment, using the UV trace to get an estimate of the percentages. Because there was a secondary metabolite also observed (2-

DMD/2016/071639

hydroxydesipramine) that could arise via two routes, a range of f_m values was estimated. It is acknowledged that the use of a human hepatocyte metabolite profile has limitations as it does not account for other clearance mechanisms that may occur *in vivo* (e.g. renal, biliary, extrahepatic metabolism). However before a new drug candidate can be administered to humans, this method is the best tool available for understanding clearance. In the case of a compound like imipramine, it is reasonable to assume that metabolism will be the clearance mechanism, due to its physicochemical properties (Varma et al., 2015).

Following its formation in liver tissues, desipramine can be subject to sequential metabolism via hydroxylation or permeate the cell membrane into the systemic circulation and the ratio of these two processes will dictate the value F_m . Since a majority of biotransformation reactions result in increased hydrophilicity, metabolites tend to decrease tissue partitioning and plasma protein binding relative to parent drugs (Obach, 2013; Smith and Obach, 2010). In this case, demethylation results in the removal of a methyl group from imipramine which is a very minor structural change and therefore has a relatively small change in its physicochemical properties. For instance, desipramine exhibits similar lipophilicity (logP of 4.6) as imipramine (logP of 4.8) (Table 1) and this is aligned with the fact that plasma protein binding is not different between imipramine and desipramine, with measured f_{up} of 0.26 and 0.21, respectively (Table 6). Desipramine displays high lipoidal permeability similar to its parent drug and both imipramine and desipramine are rapidly and completely absorbed when taken orally ($F_a > 95\%$) (Dencker et al., 1976; Sallee and Pollock, 1990). This high human absorption fraction is correlated with their high passive permeability measured in artificial membrane PAMPA (Avdeef et al., 2007; Chen et al., 2008). Therefore, in this study, the passive diffusion clearance of desipramine from the hepatocyte into the systemic circulation (39.1 mL/min/kg) was deemed to be reasonably predicted from passive permeability and hepatocyte surface area. The estimation of the systemic availability of the metabolite can help to elucidate the currently limited understanding regarding metabolite disposition, i.e. the

DMD/2016/071639

predominant metabolites *in vitro* are not the same as the predominant metabolites *in vivo*, or certain metabolites circulate once formed, whereas others do not (Smith and Dalvie, 2012; Zamek-Gliszczynski et al., 2014). These differences can be hypothesized to be associated with metabolic enzymes, as well as basolateral efflux in liver, intestine and kidney. The availability of desipramine following its formation (F_m) was estimated as 60% (Table 2), which indicates that more than a half of the desipramine generated from imipramine escapes sequential clearance and leaves the liver to enter the systemic circulation. Using all of these values extrapolated from *in vitro* data, CL_p , CL_m , f_m , and F_m , permitted an estimation of AUC_m/AUC_p for desipramine and imipramine that was in the range observed in clinical studies (Table 5).

The PBPK model built for imipramine was able to simulate the PK profile observed from clinical study following a 50 mg i.v. infusion of imipramine in EM healthy volunteers (Brøsen and Gram, 1988). Both imipramine and desipramine are basic and lipophilic compounds, and distribute widely to various tissues. The predicted V_{ss} (11 L/kg) of imipramine using Simcyp is on the low end of reported values mostly ranging from 10 to 20 L/kg (Abernethyl et al., 1984; Ciraulo et al., 1988). The predicted CL for imipramine is 9.4 mL/min/kg and consistent with the observed range of clinical values (8–15 mL/min/kg). The PBPK model for metabolite desipramine was developed using desipramine *in vitro* data. Desipramine was predicted to also have a large volume of distribution ($V_{ss} = 6.5$ L/kg) similar to its parent drug. Based on bottom-up approach with *in vitro* data as input parameters, the minimal PBPK model captured the shape of desipramine concentration-time curve successfully in both EM and PM populations following oral administration of imipramine (**Figures 7 and 9**).

Following oral dosing of imipramine to healthy subjects genotyped as CYP2D6 extensive metabolizers, the desipramine /imipramine AUC ratio was observed to range from 0.48 to 1.1 (Brøsen and Gram, 1988; Kurtz et al., 1997; Sutfin et al., 1984). Both static and dynamic PBPK models successfully provided AUC_m/AUC_p ratio estimates in reasonable agreement with reported values in EM volunteers. The $AUC_{desipramine}/AUC_{imipramine}$ was about 8 times higher in rapid EM compared with PMs

DMD/2016/071639

with a long $t_{1/2}$ for desipramine in PM volunteers (more than 2 weeks) (Brøsen et al., 1986). **For PM populations, the static and dynamic PBPK models predicted the AUC ratios within 2-fold of observed values.** These findings suggest the relevant impact of CYP2D6 activity on the metabolic disposition of imipramine and that *in vitro* methods and mechanistic modeling can reasonably predict the relative exposure of active metabolite desipramine. When considering the efficacy of imipramine in depressive patients, imipramine and desipramine concentrations should be taken as a basis for dose recommendation (Kirchheiner et al., 2001).

In conclusion, understanding sequential elimination of major metabolites is important to elucidate metabolite exposure. As shown in the present study, characterization of imipramine and its active metabolite desipramine with respect to metabolic clearance by *in vitro* methods, binding and membrane permeability properties, all coupled with static and dynamic PBPK models can provide mechanistic insight into overall pharmacokinetics and clinical relevance of genetic polymorphism on exposure to desipramine. The methods described in this work are currently employed to other drug and metabolite pairs wherein overall clearance pathways and dispositional properties are different from the example of imipramine and desipramine.

Acknowledgements

The authors would like to thank Susanna Tse, Manthena Varma, and Jian Lin for their insightful suggestions/discussion and software assistance. Hoa Nguyen is a Pfizer Worldwide Research and Development Postdoctoral Fellowship awardee.

Authorship Contributions

Participated in research design: Nguyen, Callegari, Obach

Conducted experiments: Nguyen, Obach

Performed data analysis: Nguyen, Callegari, Obach

Wrote or Contributed to writing of the manuscript: Nguyen, Callegari, Obach

References

- Abernethy DR, Greenblatt DJ and Shader RI (1984) Imipramine-cimetidine interaction: impairment of clearance and enhanced absolute bioavailability. *Journal of Pharmacology and Experimental Therapeutics* **229**:702-705.
- Abernethyl DR, Divoll M, Greenblatt DJ, Harmatz JS and Shader RI (1984) Absolute bioavailability of imipramine: influence of food. *Psychopharmacology* **83**:104-106.
- Albers LJ, Reist C, Vu RL, Fujimoto K, Ozdemir V, Helmeste D, Poland R and Tang SW (2000) Effect of venlafaxine on imipramine metabolism. *Psychiatry research* **96**:235-243.
- Avdeef A, Bendels S, Di L, Faller B, Kansy M, Sugano K and Yamauchi Y (2007) PAMPA—critical factors for better predictions of absorption. *Journal of pharmaceutical sciences* **96**:2893-2909.
- Ball SE, Ahern D, Scatina J and Kao J (1997) Venlafaxine: in vitro inhibition of CYP2D6 dependent imipramine and desipramine metabolism; comparative studies with selected SSRIs, and effects on human hepatic CYP3A4, CYP2C9 and CYP1A2. *British journal of clinical pharmacology* **43**:619-626.
- Bergstrom RF, Peyton AL and Lemberger L (1992) Quantification and mechanism of the fluoxetine and tricyclic antidepressant interaction. *Clinical Pharmacology & Therapeutics* **51**:239-248.
- Bernard S, Neville KA, Nguyen AT and Flockhart DA (2006) Interethnic differences in genetic polymorphisms of CYP2D6 in the US population: clinical implications. *The oncologist* **11**:126-135.
- Brøsen K and Gram LF (1988) First-pass metabolism of imipramine and desipramine: impact of the sparteine oxidation phenotype. *Clinical Pharmacology & Therapeutics* **43**:400-406.
- Brøsen K, Otton S and Gram LF (1986) Imipramine demethylation and hydroxylation: impact of the sparteine oxidation phenotype. *Clinical Pharmacology & Therapeutics* **40**:543-549.
- Callaghan JT, Cerimele BJ, Kassahun KJ, Nyhart EH, Hoyes-Beehler PJ and Kondraske GV (1997) Olanzapine: interaction study with imipramine. *The Journal of Clinical Pharmacology* **37**:971-978.
- Callegari E, Kalgutkar AS, Leung L, Obach RS, Plowchalk DR and Tse S (2013) Drug metabolites as cytochrome p450 inhibitors: a retrospective analysis and proposed algorithm for evaluation of the pharmacokinetic interaction potential of metabolites in drug discovery and development. *Drug Metabolism and Disposition* **41**:2047-2055.
- Chen M, Tabaczewski P, Truscott SM, Van Kaer L and Stroynowski I (2005) Hepatocytes express abundant surface class I MHC and efficiently use transporter associated with antigen processing, tapasin, and low molecular weight polypeptide proteasome subunit components of antigen processing and presentation pathway. *The Journal of Immunology* **175**:1047-1055.
- Chen X, Murawski A, Patel K, Crespi CL and Balimane PV (2008) A novel design of artificial membrane for improving the PAMPA model. *Pharmaceutical research* **25**:1511-1520.

DMD/2016/071639

- Ciraulo DA, Barnhill JG and Jaffe JH (1988) Clinical pharmacokinetics of imipramine and desipramine in alcoholics and normal volunteers. *Clinical Pharmacology & Therapeutics* **43**:509-518.
- Dahl M-L, Johansson I, Palmertz MP, Ingelman-Sundberg M and Sjöqvist F (1992) Analysis of the CYP2D6 gene in relation to debrisoquin and desipramine hydroxylation in a Swedish population. *Clinical Pharmacology & Therapeutics* **51**:12-17.
- Dencker H, Dencker S, Green A and Nagy A (1976) Intestinal absorption, demethylation, and enterohepatic circulation of imipramine. *Clinical pharmacology and therapeutics* **19**:584-586.
- Doan KMM, Humphreys JE, Webster LO, Wring SA, Shampine LJ, Serabjit-Singh CJ, Adkison KK and Polli JW (2002) Passive permeability and P-glycoprotein-mediated efflux differentiate central nervous system (CNS) and non-CNS marketed drugs. *Journal of Pharmacology and Experimental Therapeutics* **303**:1029-1037.
- FADA F (2012) Guidance for industry: drug interaction studies—study design, data analysis, implications for dosing, and labeling recommendations.
- FDA US (2008) Guidance for Industry: Safety Testing of Drug Metabolites, in <http://www.fda.gov/cder/guidance/index.htm>, Center for Drug Evaluation and Research, Rockville, MD.
- Fišar Z, Krulík R, Fuksová K and Sikora J (1996) Imipramine distribution among red blood cells, plasma and brain tissue. *Gen Physiol Biophys* **15**:51-64.
- Fujikawa M, Nakao K, Shimizu R and Akamatsu M (2007) QSAR study on permeability of hydrophobic compounds with artificial membranes. *Bioorganic & medicinal chemistry* **15**:3756-3767.
- Furman KD, Grimm DR, Mueller T, Holley-Shanks RR, Bertz RJ, Williams LA, Spear BB and Katz DA (2004) Impact of CYP2D6 intermediate metabolizer alleles on single-dose desipramine pharmacokinetics. *Pharmacogenetics and Genomics* **14**:279-284.
- Guideline E (2012) Guideline on the investigation of drug interactions, EMEA/CPMP/EWP/560/95 Rev. 1.
- Guideline IHT (2009) Guidance on nonclinical safety studies for the conduct of human clinical trials and marketing authorization for pharmaceuticals M3 (R2), in *International conference on harmonisation of technical requirements for registration of pharmaceuticals for human use*.
- Houston J and Taylor G (1984) Drug metabolite concentration-time profiles: influence of route of drug administration. *British journal of clinical pharmacology* **17**:385-394.
- Houston JB (1981) Drug metabolite kinetics. *Pharmacology & therapeutics* **15**:521-552.
- Jamei M, Dickinson GL and Rostami-Hodjegan A (2009) A framework for assessing inter-individual variability in pharmacokinetics using virtual human populations and integrating general knowledge of physical chemistry, biology, anatomy, physiology and genetics: a tale of 'bottom-up' vs 'top-down' recognition of covariates. *Drug metabolism and pharmacokinetics* **24**:53-75.
- Jones HM, Barton HA, Lai Y, Bi Y-a, Kimoto E, Kempshall S, Tate SC, El-Kattan A, Houston JB and Galetin A (2012) Mechanistic pharmacokinetic modeling for the prediction of transporter-mediated disposition in humans from sandwich culture human hepatocyte data. *Drug Metabolism and Disposition* **40**:1007-1017.
- Kirchheiner J, Brøsen K, Dahl M-L, Gram L, Kasper S, Roots I, Sjöqvist F, Spina E and Brockmüller J (2001) CYP2D6 and CYP2C19 genotype-based dose recommendations

- for antidepressants: a first step towards subpopulation-specific dosages. *Acta Psychiatrica Scandinavica* **104**:173-192.
- Koyama E, Sohn D-R, Shin S-G, Chiba K, Shin J-G, Kim Y-H, Echizen H and Ishizaki T (1994) Metabolic disposition of imipramine in oriental subjects: relation to metoprolol alpha-hydroxylation and S-mephenytoin 4'-hydroxylation phenotypes. *Journal of Pharmacology and Experimental Therapeutics* **271**:860-867.
- Kurtz DL, Bergstrom RF, Goldberg MJ and Cerimele BJ (1997) The effect of sertraline on the pharmacokinetics of desipramine and imipramine. *Clinical Pharmacology & Therapeutics* **62**:145-156.
- Leucht S, Hackl H-J, Steimer W, Angersbach D and Zimmer R (2000) Effect of adjunctive paroxetine on serum levels and side-effects of tricyclic antidepressants in depressive inpatients. *Psychopharmacology* **147**:378-383.
- Madani S, Barilla D, Cramer J, Wang Y and Paul C (2002) Effect of terbinafine on the pharmacokinetics and pharmacodynamics of desipramine in healthy volunteers identified as cytochrome P450 2D6 (CYP2D6) extensive metabolizers. *The Journal of Clinical Pharmacology* **42**:1211-1218.
- Nakajima M, Tanaka E, Kobayashi T, Ohashi N, Kume T and Yokoi T (2002) Imipramine N-glucuronidation in human liver microsomes: biphasic kinetics and characterization of UDP-glucuronosyltransferase isoforms. *Drug metabolism and disposition* **30**:636-642.
- Naritomi Y, Terashita S, Kagayama A and Sugiyama Y (2003) Utility of hepatocytes in predicting drug metabolism: comparison of hepatic intrinsic clearance in rats and humans in vivo and in vitro. *Drug Metabolism and Disposition* **31**:580-588.
- Nguyen HQ, Kimoto E, Callegari E and Obach RS (2016) Mechanistic Modeling to Predict Midazolam Metabolite Exposure from In Vitro Data. *Drug Metabolism and Disposition* **44**:781-791.
- Obach R (2011) Predicting clearance in humans from in vitro data. *Current topics in medicinal chemistry* **11**:334-339.
- Obach RS (1997) Nonspecific binding to microsomes: impact on scale-up of in vitro intrinsic clearance to hepatic clearance as assessed through examination of warfarin, imipramine, and propranolol. *Drug Metabolism and Disposition* **25**:1359-1369.
- Obach RS (1999) Prediction of human clearance of twenty-nine drugs from hepatic microsomal intrinsic clearance data: an examination of in vitro half-life approach and nonspecific binding to microsomes. *Drug Metabolism and Disposition* **27**:1350-1359.
- Obach RS (2013) Pharmacologically active drug metabolites: impact on drug discovery and pharmacotherapy. *Pharmacological reviews* **65**:578-640.
- Pang KS (1985) A review of metabolite kinetics. *Journal of pharmacokinetics and biopharmaceutics* **13**:633-662.
- Potter WZ, Calil HM, Sutfin TA, Zavadil AP, Jusko WJ, Rapoport J and Goodwin FK (1982) Active metabolites of imipramine and desipramine in man. *Clinical Pharmacology & Therapeutics* **31**:393-401.
- Poulin P and Theil FP (2000) A priori prediction of tissue: plasma partition coefficients of drugs to facilitate the use of physiologically-based pharmacokinetic models in drug discovery. *Journal of pharmaceutical sciences* **89**:16-35.

DMD/2016/071639

- Rodgers T and Rowland M (2006) Physiologically based pharmacokinetic modelling 2: predicting the tissue distribution of acids, very weak bases, neutrals and zwitterions. *Journal of pharmaceutical sciences* **95**:1238-1257.
- Rowland M, Peck C and Tucker G (2011) Physiologically-based pharmacokinetics in drug development and regulatory science. *Annual review of pharmacology and toxicology* **51**:45-73.
- Sallee F and Pollock B (1990) Clinical pharmacokinetics of imipramine and desipramine. *Clinical pharmacokinetics* **18**:346-364.
- Schenk P, Van Fessem M, Verploegh-Van Rij S, Mathot R, van Gelder T, Vulto A, van Vliet M, Lindemans J, Bruijn JA and van Schaik R (2008) Association of graded allele-specific changes in CYP2D6 function with imipramine dose requirement in a large group of depressed patients. *Molecular psychiatry* **13**:597-605.
- Skjelbo E, Brøsen K, Hallas J and Gram LF (1991) The mephenytoin oxidation polymorphism is partially responsible for the N-demethylation of imipramine. *Clinical Pharmacology & Therapeutics* **49**:18-23.
- Smith DA and Dalvie D (2012) Why do metabolites circulate? *Xenobiotica; the fate of foreign compounds in biological systems* **42**:107-126.
- Smith DA and Obach RS (2010) Metabolites: have we MIST out the importance of structure and physicochemistry? *Bioanalysis* **2**:1223-1233.
- Spigset O, Granberg K, Hägg S, Norström Å and Dahlqvist R (1997) Relationship between fluvoxamine pharmacokinetics and CYP2D6/CYP2C19 phenotype polymorphisms. *European journal of clinical pharmacology* **52**:129-133.
- Spina E, Gitto C, Avenoso A, Campo G, Caputi A and Perucca E (1997) Relationship between plasma desipramine levels, CYP2D6 phenotype and clinical response to desipramine: a prospective study. *European journal of clinical pharmacology* **51**:395-398.
- St-Pierre MV, Xu X and Pang KS (1988) Primary, secondary, and tertiary metabolite kinetics. *Journal of pharmacokinetics and biopharmaceutics* **16**:493-527.
- Sugano K, Kansy M, Artursson P, Avdeef A, Bendels S, Di L, Ecker GF, Faller B, Fischer H and Gerebtzoff G (2010) Coexistence of passive and carrier-mediated processes in drug transport. *Nature reviews Drug discovery* **9**:597-614.
- Sutfin TA, DeVane CL and Jusko WJ (1984) The analysis and disposition of imipramine and its active metabolites in man. *Psychopharmacology* **82**:310-317.
- Swanson JR, Jones GR, Krasselt W, Denmark LN and Ratti F (1997) Death of two subjects due to imipramine and desipramine metabolite accumulation during chronic therapy: a review of the literature and possible mechanisms. *Journal of forensic sciences* **42**:335-339.
- Varma MV, Steyn SJ, Allerton C and El-Kattan AF (2015) Predicting clearance mechanism in drug discovery: extended clearance classification system (ECCS). *Pharmaceutical research* **32**:3785-3802.
- Vieira MdL, Kim MJ, Apparaju S, Sinha V, Zineh I, Huang SM and Zhao P (2014) PBPK model describes the effects of comedication and genetic polymorphism on systemic exposure of drugs that undergo multiple clearance pathways. *Clinical Pharmacology & Therapeutics* **95**:550-557.

DMD/2016/071639

- Wells B, Pieper J, Self T, Stewart C, Waldon S, Bobo L and Warner C (1986) The effect of ranitidine and cimetidine on imipramine disposition. *European journal of clinical pharmacology* **31**:285-290.
- Yeung CK, Fujioka Y, Hachad H, Levy RH and Isoherranen N (2011) Are Circulating Metabolites Important in Drug-Drug Interactions? Quantitative Analysis of Risk Prediction and Inhibitory Potency. *Clinical Pharmacology & Therapeutics* **89**:105-113.
- Yu H and Tweedie D (2013) A perspective on the contribution of metabolites to drug-drug interaction potential: the need to consider both circulating levels and inhibition potency. *Drug Metabolism and Disposition* **41**:536-540.
- Zamek-Gliszczyński MJ, Chu X, Polli JW, Paine MF and Galetin A (2014) Understanding the transport properties of metabolites: case studies and considerations for drug development. *Drug Metabolism and Disposition* **42**:650-664.
- Zhang Z and Kaminsky LS (2007) Determination of metabolic rates and enzyme kinetics. *Drug Metabolism in Drug Design and Development*:413.
- Zhou D, Guo J, Linnenbach AJ, Booth-Genthe CL and Grimm SW (2010) Role of human UGT2B10 in N-glucuronidation of tricyclic antidepressants, amitriptyline, imipramine, clomipramine, and trimipramine. *Drug Metabolism and Disposition* **38**:863-870.

DMD/2016/071639

Figure Legends

Figure 1: HPLC–UV traces of imipramine extracts of human hepatocyte incubations. A is the UV chromatogram of the control incubation without parent drug. B is the UV chromatogram of imipramine incubation. The wavelength represented is $\lambda = 280$ nm.

Figure 2: Proposed pathway of imipramine metabolism and corresponding f_m calculated from HPLC–UV traces of imipramine extracts.

Figure 3: The formation of desipramine from imipramine in human hepatocytes. Each point represents the mean of triplicate measurements with standard error bar. Line represents the best fit according to the model expressed by equation 11.

Figure 4: Percent of imipramine remaining in hepatocyte incubation (mean values and standard error bars of triplicate measurements) and fitted exponential depletion curve.

Figure 5: Percent of desipramine remaining in extensive metabolizer (left) and poor metabolizer (right) microsomal incubations (mean values and standard error bars of triplicate measurements) and fitted exponential depletion curve.

Figure 6: Simulations of imipramine and desipramine metabolite mean plasma concentration-time profiles after a **normalized i.v. dose of 1mg** imipramine in CYP2D6 EM Subjects. The points represent **1 mg dose normalized** observed mean values. The continuous lines represent the mean predicted values from individual trials (10 x 50; 20 – 50 years; 50% Female).

Figure 7: Simulations of imipramine and desipramine metabolite mean plasma concentration-time profiles after a **normalized oral dose of 1 mg** imipramine in CYP2D6 EM Subjects. The points represent **1 mg dose normalized** observed mean values. The continuous lines represent the mean predicted values from individual trials (10 x 50; 20 – 50 years; 50% Female).

DMD/2016/071639

Figure 8: Simulations of imipramine and desipramine metabolite mean plasma concentration-time profiles after a **normalized i.v. dose of 1mg** of imipramine in CYP2D6 PM Subjects. The points represent **1 mg** dose normalized observed mean values. The continuous lines represent the mean predicted values from individual trials (10 x 50; 20 – 50 years; 50% Female).

Figure 9: Simulations of imipramine and desipramine metabolite mean plasma concentration-time profiles after a **normalized oral dose of 1 mg** of imipramine in CYP2D6 PM Subjects. The points represent **1 mg dose** normalized observed mean values. The continuous lines represent the mean predicted values from individual trials (10 x 50; 20 – 50 years; 50% Female).

DMD/2016/071639

Tables

Table 1. Parameters for imipramine and active metabolite desipramine in PBPK model

Parameter	Imipramine	Desipramine	Source
Molecular Weight (g/mol)	280.4	266.4	ACD
logP	4.8	4.57	ACD
Compound Type	Base	Base	ACD
pK _a	9.45	10.26	ACD
B/P	1.02	1.16	(Ciraulo et al., 1988)
f _{u,p}	0.26	0.21	Measured
Absorption			
Model	First-order	n/a	
Fraction absorbed	1	n/a	(Sallee and Pollock, 1990)
k _a (h ⁻¹)	1	n/a	Simcyp default
f _{u,gut}	1	n/a	Assumed
MDCK-II (10 ⁻⁶ cm/s)	39.3	n/a	(Doan et al., 2002)
Distribution			
Model	Minimal PBPK	Minimal PBPK	
V _{ss} (L/kg)	11	6.5	Predicted using method 2 (Rodgers and Rowland, 2006)
Elimination			
Enzyme Kinetics (CL _{int}) (μL/min/mg protein)	9.12	22	Measured
Additional CL (Hep CL _{int}) (μL/min/10 ⁶ cells)	8	0	Measured
f _{u,inc}	0.42	0.39	Measured
CL _{renal} (L/hr)	0.15	1.0	(Ciraulo et al., 1988)

ACD: values calculated using Advanced Chemistry Development (ACD/Labs) Software V12.5

DMD/2016/071639

Table 2: List of metabolites observed *in vitro* and corresponding calculated f_m , $f_{CL,m}$

Metabolite	UV Peak Area	f_m	$f_{CL,m}$
Desipramine	45021	0.44	0.44 - 0.62
Imipramine N-glucuronide	18764	0.18	0.18
Hydroxyimipramine	20339	0.2	0.20 - 0.38
Hydroxydesipramine	18498	0.18	
All metabolites	102622	1	

DMD/2016/071639

Table 3: Predicted Values for CL_H , F_h , $CL_{int,pass}$, F_m

Substrate	CL_H (mL/min/kg)	F_h	$CL_{int,pass}$ (mL/min/kg)	F_m
Imipramine	9.4	0.55	-	-
Desipramine (in EM)	6.4	-	39.1	0.60
Desipramine (in PM)	1.0	-	39.1	0.93

DMD/2016/071639

Table 4: Predicted AUC ratios

Route	AUC _{desipramine} /AUC _{imipramine}					
	CYP2D6 EM population			CYP2D6 PM population		
	Static Model	PBPK	Observed	Static Model	PBPK	Observed
i.v	0.39 – 0.54	0.19 – 0.28	0.21 – 0.46 ^a	7.0	3.7 – 5.0	
p.o	0.69 – 0.98	0.32 – 0.54	0.48 – 1.1	12.6	6.5 – 9.1	2.8 – 6.8
Reference	(Abernethy et al., 1984; Albers et al., 2000; Bergstrom et al., 1992; Brøsen et al., 1986; Callaghan et al., 1997; Koyama et al., 1994; Kurtz et al., 1997; Skjelbo et al., 1991; Sutfin et al., 1984; Wells et al., 1986)			(Brøsen et al., 1986; Koyama et al., 1994)		

^a Observed value range was obtained from Sutfin et al. study (Sutfin et al., 1984), in which single intramuscular (i.m) doses of imipramine were administered to healthy volunteers.

DMD/2016/071639

Table 5: Simcyp mean predicted pharmacokinetic parameters of imipramine and desipramine in plasma following i.v administration of imipramine (normalized dose of 1 mg) in CYP2D6 EM and PM populations

Parameter	Imipramine	Desipramine	
	EM	EM	PM
CL (mL/min/kg)	9.4 (8 – 15) ^a	-	-
V _{ss} (L/kg)	11 (10 – 20) ^a	6.5 (10 – 50) ^a	6.5
AUC (ng/mL.hr)	28 (12 – 22) ^a	6.8 (3.7 – 6.9) ^a	120

^aData represented as predicted mean of whole population and range of observed values in parenthesis

DMD/2016/071639

Table 6: Simcyp mean predicted pharmacokinetic parameters of imipramine and desipramine in plasma following oral administration of imipramine (normalized dose of 1 mg) in CYP2D6 EM and PMs

Parameter	Imipramine	Desipramine	
	EM	EM	PM
C _{max} (ng/mL)	0.46 – 0.6 (0.35 – 0.60) ^a	0.12 – 0.18	0.32 – 0.42
T _{max} (hr)	2.9 – 3.6 (2.7 – 5.1) ^a	3.6 – 5.1	39 – 46
AUC (ng/mL.hr)	12 – 15 (4.9 – 10) ^a	4.3 – 6.9 (4.1 – 11.2) ^a	86 – 116
F _h	0.55	-	-
F	0.48 (0.22-0.80) ^a	-	-

^aData represented as predicted range of individual trial means and range of observed values in parenthesis (Ciraulo et al., 1988; Koyama et al., 1994; Kurtz et al., 1997; Sutfin et al., 1984))

Figures

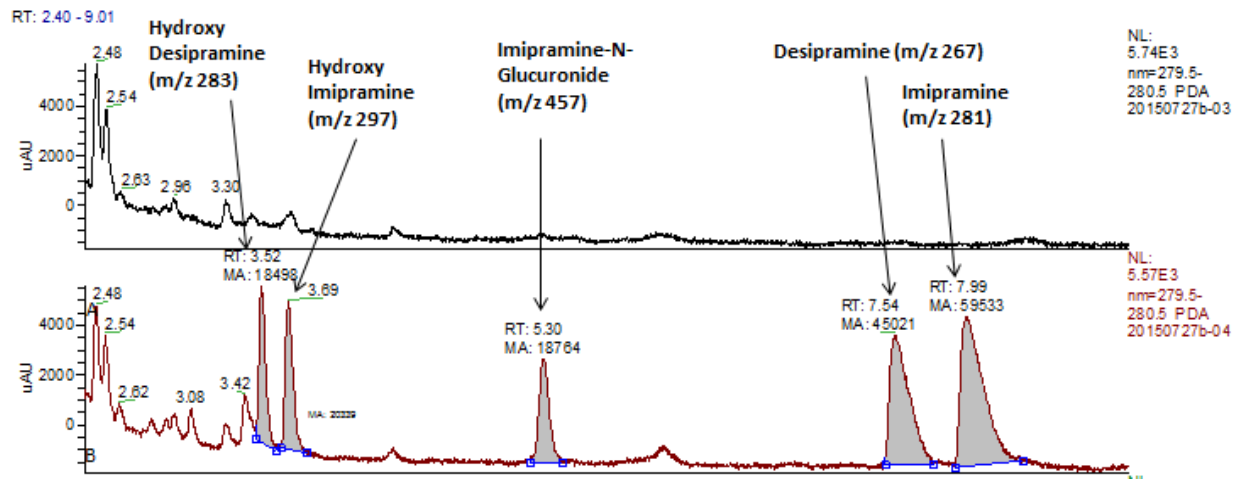


Figure 1

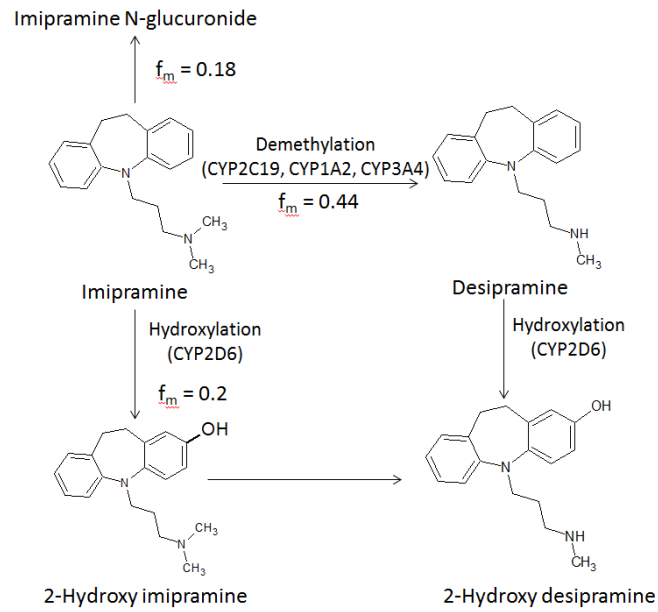


Figure 2

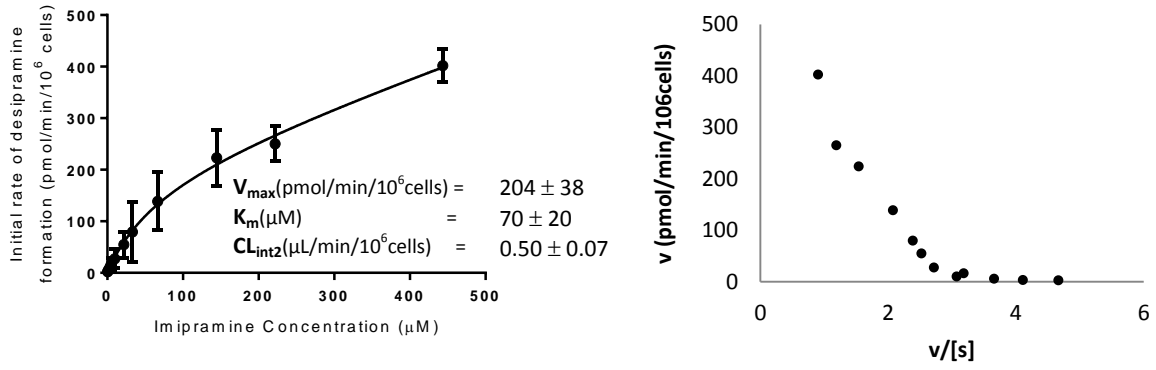


Figure 3

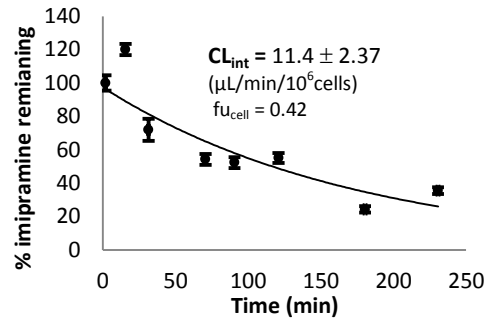


Figure 4

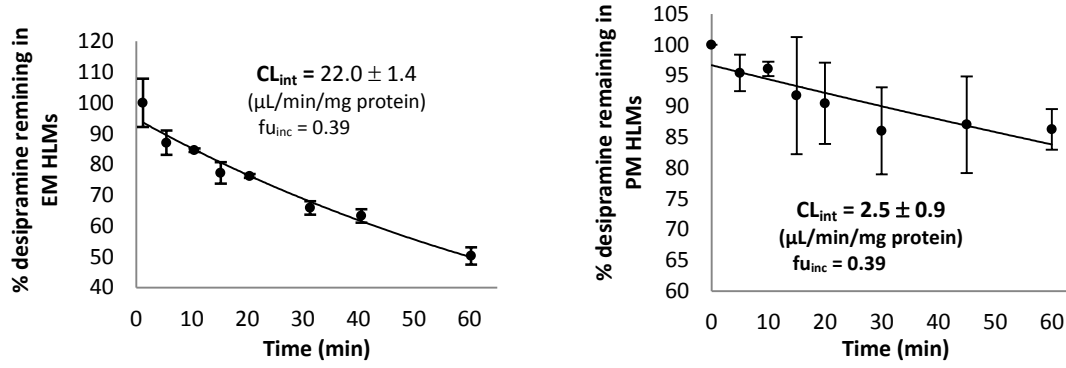


Figure 5

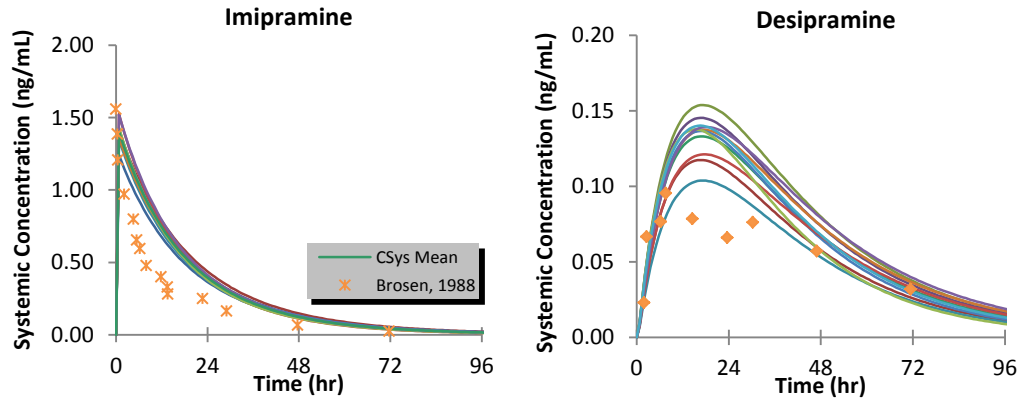


Figure 6

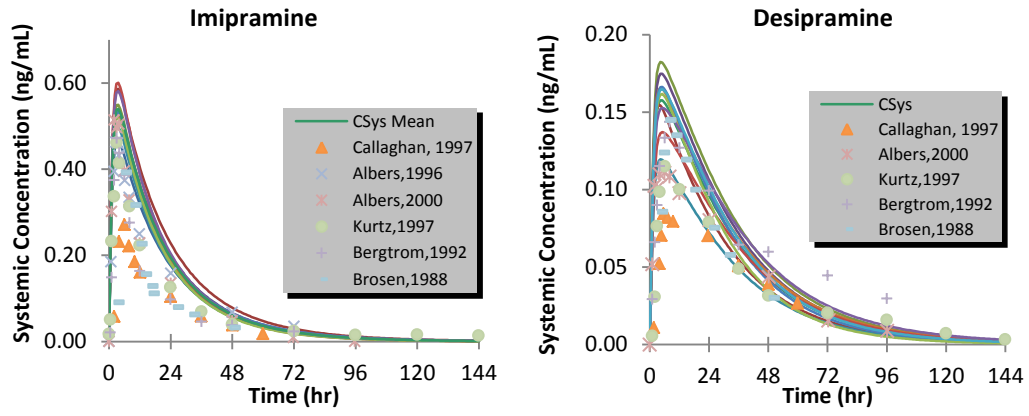


Figure 7

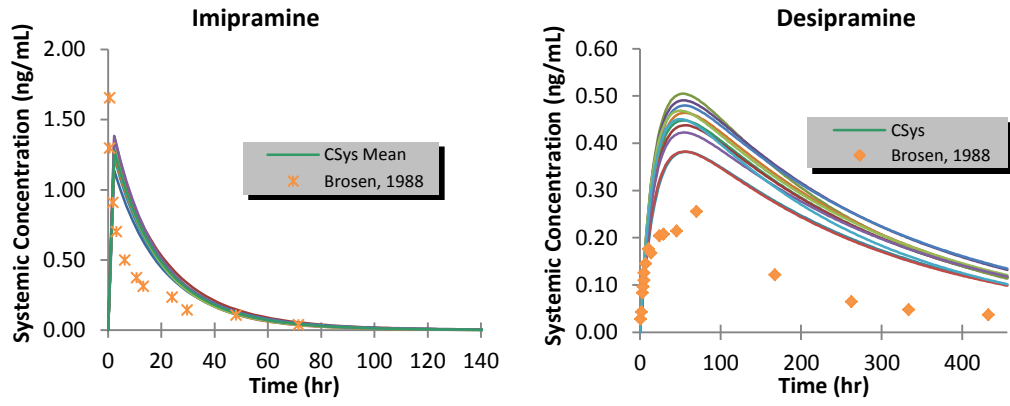


Figure 8

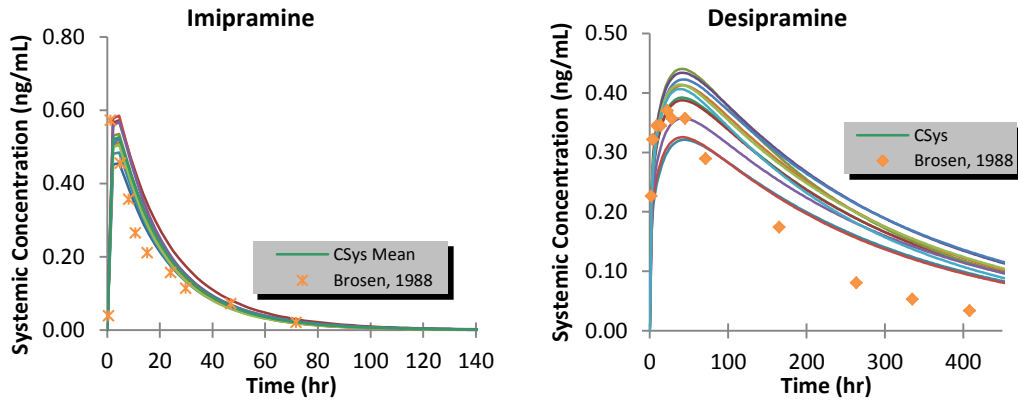


Figure 9